Environ. Sci. Technol. **2004**, *38,* 5164−5169

Laboratory Assessment of the Mobility of Nanomaterials in Porous Media

HÉLÈNE F. LECOANET,[†] JEAN-YVES BOTTERO,[‡] AND MARK R. WIESNER*,[†]

Department of Civil and Environmental Engineering, Rice University, MS-317, 6100 Main Street, Houston, Texas 77005, and CEREGE, CNRS-UMR 6635, University of Aix-Marseille III, Europôle Méditerranéen de l'Arbois, BP 80, 13545 Aix-en-Provence Cedex 04, France

The production of significant quantities of engineered nanomaterials will inevitably result in the introduction of these materials to the environment. Mobility in a well-defined porous medium was evaluated for eight particulate products of nanochemistry to assess their potential for migration in porous media such as groundwater aquifers and water treatment plant filters. Contrary to the assertion that nanomaterials present monolithic environmental risks, here we show that these nanomaterials exhibit widely differing transport behaviors. Fullerene-based nanomaterials that had been functionalized to facilitate dispersal in water displayed the highest mobilities, with a calculated potential to migrate approximately 10 m in unfractured sand aquifers. Colloidal aggregates of C_{60}, which have been the focus of recent toxicity studies, were among the least mobile of the nanomaterials evaluated.

Introduction

Estimates of the size of the current nanotechnology market range from 30 to 45 billion dollars (*1*). Although these estimates reflect uncertainty in predicting the commercialization of an emerging technology, there is little doubt that some portion of the materials marketed as products of a successful nanochemistry industry will ultimately find their way into our environment. The long list of near-term, commercial applications of nanomaterials includes many examples of common consumer products such as nano-engineered titania particles for sunscreens and paints; carbon nanotube composites in tires; silica nanoparticles as solid lubricants; and alumina nanoparticles in shampoos, detergents, and antiperspirants. The introduction of catalytic nanoparticles to groundwater has been tested for the purpose of remediating contamination (*2*). In this latter instance, the mobility of nanoparticles was considered to be a key limitation in their deployment. Moreover, the environmental implications associated with these materials are currently unknown.

A risk assessment of the potential impacts on health and environment that the production, use, and disposal of nanomaterials may engender requires information concerning both the potential for exposure to a given material and (once exposed) potential impacts such as toxicity or mutagenicity. In this work, we address the issue of nanomaterial exposure and transport in experiments designed to assess their potential for migration in porous media such as groundwater aquifers and water treatment plant filters. Here we quantify the mobility in a well-defined porous medium for eight nanomaterials currently marketed as products of nanochemistry. Laboratory observations are used to assess the potential for transport of particulate nanomaterials in a natural porous media such as a sandy groundwater aquifer.

Quantification of Particle Mobility in Porous Media

The relative mobility of a particle entrained by flow through a porous medium is linked to its tendency to deposit on immobile surfaces such as sand grains or claysin aquifers. The process of particle deposition is often considered as a sequence of particle transport to the immobile surface or "collector" followed by attachment (*3*).

Particle Transport. Particles are transported to the surface of a collector when fluid streamlines, as described for example by the Happel model (*4*), pass sufficiently close to the collector surface such that particles make contact with the surface. Particles entrained by the fluid flow may also contact collectors if they cross streamlines within a critical region due to the effects of gravity or Brownian diffusion. Transport of engineered nanoparticles and nanoscale particles will be dominated by Brownian diffusion. Forces such as the London−van der Waals and double-layer forces (e.g., the classic Derjaguin, Landau, Verwey, and Overbeek or DLVO theory; *5*, *6*) are typically considered as influencing particle attachment rather than transport. Particle trajectory calculations have been combined with the analytical solution for Brownian transport to yield closed-form solutions for the transport of particles to the surface of spherical collectors (*7*, *8*) expressed as the theoretical single collector efficiency, η_0. Data for the deposition of particles varying in size over several orders of magnitude (including particles dominated by Brownian transport) have been found to be adequately represented by this model for particle transport when conditions favor particle attachment (*9*−*13*). However, when particle attachment is not favorable, only a fraction of the collisions with the collector surface will result in particle deposition and the single collector efficiency must be modified.

Particle Attachment. The ratio of the rate of particle deposition on a collector to the rate of collisions with that collector is referred to as the collision efficiency or attachment efficiency factor, α. The attachment efficiency is a function of numerous phenomena including van der Waals forces, electrical double-layer interactions, steric interactions, hydration forces, and particle/surface hydrophobicity. The value of α is unity when there are no barriers to particle deposition and attachment is favored but may exceed 1 if phenomena at small separation distances draw particles to the surface (*14*).

Particle transport and attachment are often represented as the product of the attachment efficiency and the collector efficiency:

$$\eta_r = \alpha\eta_0 \quad (1)$$

Currently, there are no satisfactory models to describe attachment efficiency. Simple models such as DLVO theory, which consider the net particle interaction potential as a function of distance separating particles and collector surfaces due to London−van der Waals forces and electric

* Corresponding author e-mail: wiesner@rice.edu; telephone: (713)348-5129; fax: (713)348-5203.
[†] Rice University.
[‡] University of Aix-Marseille III.

10.1021/es0352303 CCC: $27.50
Published on Web 08/25/2004

TABLE 1. Characteristics of Nanomaterials Used for Filtration Experiments and Calculated Particle Mobility in a System Resembling a Sandy Groundwater Aquifer[a]

nanomaterial	size (nm)	electrophoretic mobility (10^{-8} $m^2 s^{-1} V^{-1}$)	C/C_0 ± 2 SD	α ± 2 SD	log α	distance to reduce C/C_0 to 0.1% (m)[b]
fullerol	1.2, M	not detectable	0.99 ± 0.01	(0.0001 ± 0.0001)	−3.98	14
SWNT	0.7−1.1[c] × 80−200, P (d_h = 21 nm[d])	−3.98	0.94 ± 0.01	(0.001 ± 0.0004)	−2.89	10
silica	57, M	−1.95	0.97 ± 0.01	0.008 ± 0.003	−2.10	2.4
alumoxane	74, P	−2.45	0.85 ± 0.02	0.039 ± 0.001	−1.32	0.6
silica	135, M	−2.58	0.68 ± 0.01	0.169 ± 0.004	−0.77	0.2
n-C_{60}	168, M	−1.99	0.56 ± 0.06	0.298 ± 0.013	−0.52	0.1
anatase	198, P	−0.27	0.56 ± 0.01	0.336 ± 0.005	−0.47	0.1
ferroxane	303, P	−0.43	0.30 ± 0.03	0.895 ± 0.023	−0.05	0.1

[a] M, monodisperse suspensions; P, polydisperse suspensions. [b] Conditions assumed for calculations: T = 15 °C, $H = 10^{-20}$ J, Darcy velocity = 0.003 cm/s, porosity = 0.30, mean sand grain diameter = 350 μm. [c] According to the model cross-section of an individual fullerene nanotube encased in a close-packed cylindrical surfactant micelle (*16*), the outer diameter of this nanomaterial is close to 4 nm with a specific gravity of approximately 1.0. [d] Average hydrodynamic diameter.

double-layer interaction forces, suggest that particle attachment under unfavorable conditions should be a strong function of particle size and ionic strength. However, experimental evidence does not support these predictions.

Moreover, models describing attachment efficiency, such as those that consider the balance between electrostatic and van der Waals forces, typically describe changes over length scales that may be many nanometers in size. Similarly, structural or hydration forces and steric interactions that affect particle stability may be important over length scales that are large by comparison with some nanoparticle dimensions. Extensions or modifications of current theory may be needed to describe the attachment efficiency for some smaller nanomaterials.

As an alternative to calculating attachment efficiency from first principles, the attachment efficiency may be treated as an empirical parameter that captures all aspects of particle deposition not described by the more extensively validated particle transport models; assuming that sequential steps of transport and attachment are adequate to describe particle deposition. A mass balance of particles over a differential volume of porous medium can be integrated over distance within a homogeneous medium to yield an expression for the attachment efficiency factor, α (*9*):

$$\alpha = -\frac{2d_C}{3(1-\epsilon)\eta_0 L}\ln(C/C_0) \qquad (2)$$

where d_C is the diameter of a collector (assumed to be spherical) in the porous medium, ϵ is the porosity of the porous medium, L is the length of the porous medium, C and C_0 are respectively the particle concentrations present at distance L and at $L = 0$, and η_0 is the clean bed single collector efficiency that describes the particle transport to an individual collector before particle accumulation alters the collector geometry. The clean bed collector efficiency can be calculated as function of the Darcy velocity, porous medium grain size, porosity, and temperature among other variables (*7*, *8*).

Using experimental C/C_0 values (fraction of influent particles remaining) and theoretical η_0 values, experimental α values can be calculated for a given particle suspension. Theoretically, values of the attachment efficiency calculated from data obtained from experiments with one porous medium can be applied to another porous medium of similar composition but different grain size, fluid flow rate, and porosity. Although the validity of interpretting C/C_0 data to obtain an estimate of attachment efficiency has been established for nanoscale particles (e.g., refs *11*−*14*), this assumption has not yet been evaluated for engineered nanoparticles.

Materials and Methods

Filter Medium. The porous medium used in these experiments was spherical glass beads (Particle Technology Ltd., Hatton, Derbyshire, UK) in a size range of 300−425 μm, with a mean diameter of 355 μm. They were passed through U.S. 50 (300 μm) and U.S. 40 (425 μm) sieves, and those beads retained on the U.S. 50 sieve were used as the porous medium. The beads were cleaned using the procedure outlined by Tobiason and O'Melia (*12*). The beads were tightly packed into a 9.25 cm cylindrical acrylic column supported on a Nylon Spectra/Mesh screen yielding a porosity of 0.43.

Nanomaterials. Eight types of nanoparticles were studied: silica (2 sizes), anatase, ferroxane, alumoxane, fullerol (hydroxylated C_{60}), clusters of C_{60} referred to as *n*-C_{60}, and single-wall carbon nanotubes. Selected physicochemical characteristics of these nanomaterials are summarized in Table 1. Particle size (with the exception of the fullerol particles) was determined by photon correlation spectroscopy (PCS system 4700c, Malvern Instruments Inc., South Borough, MA). Measurements of size for the silica nanoparticles yielded values that coincided closely with those provided by the manufacturer (Nissan Chemical Industries Ltd., Tarrytown, NY; 47 nm (Snowtex OL) and 103 nm (Snowtex ZL)). However, the diameter of anatase was approximately five times that provided by the manufacturer (Altair Nanomaterials Inc., Reno, NV; 40 nm (TiNano40)). Electron microscope imagery established that this discrepancy was due to the formation of aggregates that did not change in size over time as monitored by PCS (Figure 1).

Ferroxane particles (ferroxane-AA), approximately 300 nm in diameter, were formed following the method previously develop in our laboratory (*15*). Ferroxanes consist of an FeOOH core with the structure of the lepidocrocite coated with acetic acid. Alumoxanes have an analogous structure (*16*) and in this case were formed from a reaction of boehmite $[Al(O)(OH)]_n$ with acetic acid. PCS measurements of the alumoxanes prepared in this work indicated a mean diameter of 74 nm.

Fullerol particles (C_{60} hydroxide, $C_{60}(OH)_m$, m = 22−26) and fullerene C_{60} (99.5+% purity) were obtained from MER Corporation (Tucson, AZ). Whereas fullerol is a water-soluble fullerene with an outer diameter equal to that of a spherical buckyball (about 1.2 nm in diameter), fullerene C_{60} is virtually insoluble in water. We used a preparation procedure similar to that described by Scrivens et al. (*17*) for producing fine aqueous suspensions of C_{60} clusters starting from a solution in benzene that is added to water resulting in 95% of the C_{60} present as clusters between 250 and 350 nm when the benzene is evaporated. In our work, we made *n*-C_{60} suspensions from a concentrated solution of C_{60} (0.15 mg) in toluene

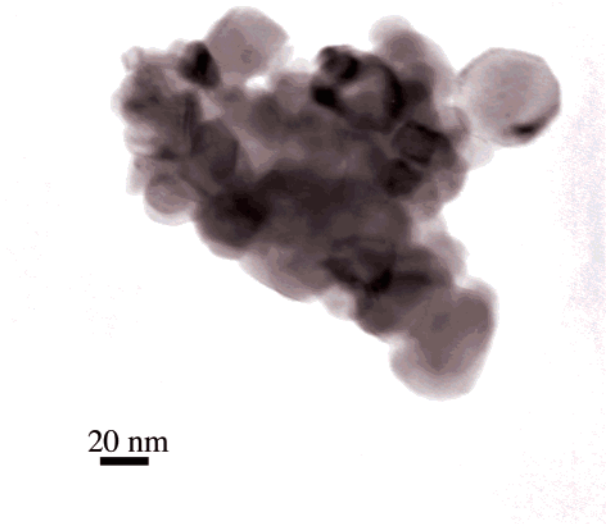

FIGURE 1. TEM picture of an anatase aggregate.

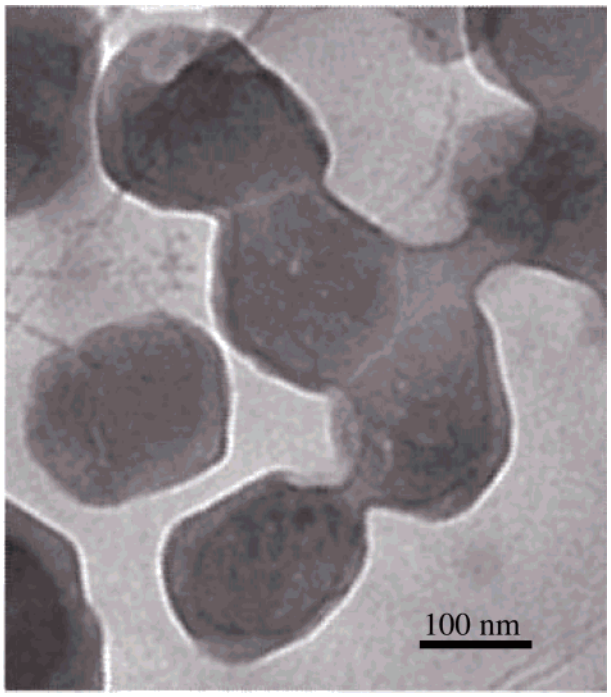

FIGURE 2. TEM image of an aggregate of C60 particles (n-C_{60}). Apparent connections between aggregates are an artifact of the nanoplast resin used in the grid preparation process.

(100 μL) to which THF (10 mL) and acetone (100 mL) were added. After addition of this mixture to water (150 mL) and evaporation of the organic solvents, we obtained aqueous suspensions of n-C_{60} with a highly uniform size of 168 ± 33 nm (Figure 2) corresponding to a value of n on the order of 10^6 depending on assumptions made for water orientation within the aggregate.

Single-wall carbon nanotubes (SWNTs) were produced at Rice University, from high-pressure CO reactor, the HiPco Process (*18*). The SWNTs were dispersed in water by using dodecylbenzene sulfonic acid, sodium salt (SDBS, provided by Aldrich) as an aqueous surfactant, following the method presented by O'Connell et al. (*19*). This procedure has a yield of over 65% solubilzed nanotubes. The resulting nanotube solution is stable for months. Their sizes were 0.7−1.1 nm in diameter and 80−200 nm long, with an average diameter of 0.9 nm and an average length of 130 nm. A mean diameter of 21 nm was determined for these carbon nanotubes by PCS, which averages diameter over all random orientations of the nanotubes. This orientation-averaged hydrodynamic diameter compares favorably with the calculated radii of gyration for tubes of these lengths and diameters.

TABLE 2. Physical and Chemical Parameters Held Constant in Experiments

parameter	value
filter media length, L	9.25 cm
column inner diameter, D	25 mm
collector diameter, d_C	355 μm
total porosity, ϵ	0.43
pore volume of column, V_p	20 mL
flow rate	12 mL/min
Darcy velocity, V	0.04 cm/s
ionic strength (NaCl)	0.01 M
pH	7.0
collector zeta potential, ζ_C	−29.8 mV
initial particle concentration, C_0	10 mg/L
temperature	21−22 °C

Electrophoretic mobilities (Table 1) of nanoparticles were measured at 22 °C, pH 7, and an ionic strength of 0.01 M using a ZetaPALS (Brookhaven Instruments Corporation, Holtsville, NY). Under these experimental conditions (Table 2), all particles and the glass beads were negatively charged. A mean value of −29.8 mV for the ζ potential of the silicate beads was obtained from streaming potential measurements (ZetaCAD, Laval Lab Inc., Laval, Canada).

Experimental Procedure. Our experiments were conducted at an ionic strength of 0.01 M (NaCl), with the pH buffered to a value of 7 by addition of 5×10^{-5} M $NaHCO_3$. These values of pH and ionic strength were selected to be within a range typical of many freshwater aquifers (*20*). Particles were introduced as a step function from 0 to 10 mg/L in the flow entering the column of porous medium. Flow was controlled at a Darcy velocity of 0.04 cm/s. Deionized water from Milli-Q water system (Millipore Corporation, Bedford, MA) used in all experiments was degassed by boiling and storing in a closed Nalgene container. Aqueous suspensions of nanoparticles were pumped through the packed bed of silicate beads at a flow rate of 12 mL/min (Darcy velocity 0.04 cm/s) provided by a magnetic-drive gear pump (Ismatec variable speed pump drive and micropump head N-07002-27, Cole-Parmer Instrument Company, Chicago, IL) through Nalgene tubing. A 2 L Pyrex beaker with cover was used as supply tank. Chemicals were mixed using a magnetic stirrer and a Teflon-coated stir bar. A flowmeter (Cole-Parmer Instrument Company, Chicago, IL) was used to monitor the flow rate. A syringe Infusion Pump 22 was used to inject the nanoparticle suspensions into the main flow just above the column. Two polypropylene syringes (Monoject, 140 mL) were loaded with nanoparticle solutions. A small magnetic stir bar was placed inside the syringes to maintain a homogeneous suspension during the course of the experiments. Syringe pumps were operated at a flow of 2 mL/min when particles were injected into the main flow. Effluent was collected at the bottom of the column. A scheme of the experimental setup is illustrated in Figure 3.

All column experiments were performed twice or more. At least 10 pore volumes of the 0.01 M NaCl electrolyte feed solution, filtered through a 0.2 μm track-etched membrane (Nucleopore) were initially passed through the porous medium and left in contact for 1 h to ensure compaction and equilibration of the bed with the influent solution. Care was

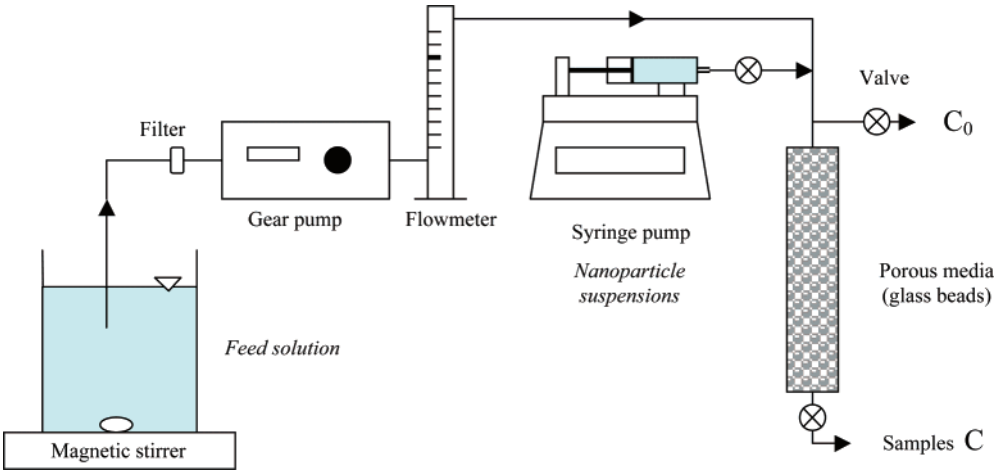

FIGURE 3. Scheme of the experimental setup.

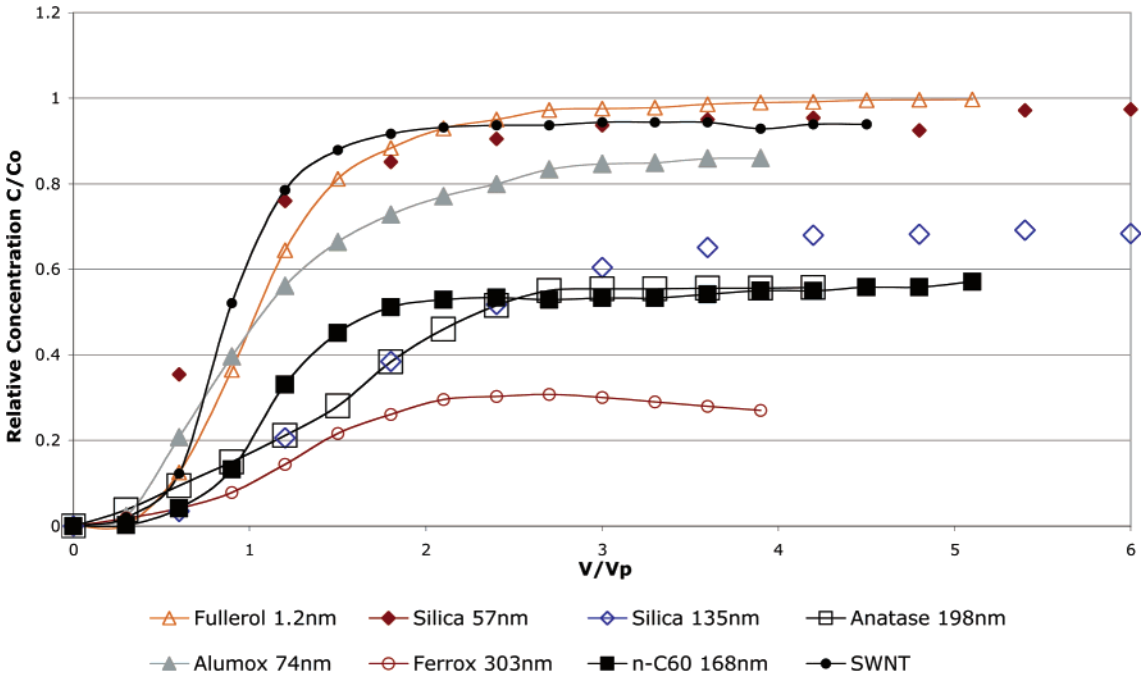

FIGURE 4. Breakthrough curves of nanoparticle suspension, showing the change in normalized effluent nanoparticle concentration (C/C_0) as a function of cumulative volume normalized to pore volume (V/V_p). Physical and chemical conditions maintained during experiments are summarized in Table 2.

taken to bleed any air remaining in the system while passing the particle-free, de-gassed solution of electrolyte through the column. Particle concentrations in the effluent were measured at discrete intervals using a U-2000 double-beam UV/Vis spectrophotometer (Hitachi Instruments Inc., Naperville, IL). Wavelength scan and calibration curve were previously determined for each of the nanomaterials used.

During the course of an experiment, the concentration of the nanomaterial introduced to the column, C_0, and the concentrations exiting the column, C, were monitored to obtain a breakthrough curve of C/C_0 as a function of the number of pore volumes passing through the porous medium. A steady plateau value of C/C_0 achieved after 2−4 pore volumes is then interpretted using eq 2 to obtain an estimate of the particle attachment efficiency.

Transmission Electronic Microscopy. TEM was done on a JEOL 2010Fastem apparatus equipped with a JEOL EM21010 single-tilt stage. TEM anatase samples were prepared by evaporating several drops of a dilute suspension of the TiNano40 onto a 300-mesh copper grid (Electron Microscopy Sciences, Fort Washington, PA). The *n*-C_{60} was deposited directly by ultracentrifugation on 200-mesh Cu Formvar carbon grid precoated with a water-soluble melamine resin (Nanoplast FB101, Ted Pella Inc., Redding, CA). The sample was ultracentrifuged at 25000 rpm for 16 h at 10 °C using a Beckman Coulter Optima LE-80K ultracentrifuge and swinging-buckets rotor (Rotor Sorvall TH-641).

Results and Discussion

Breakthrough curves and thus mobilities of the materials evaluated in this study differed substantially from one another (Figure 4). Among the fullerene-based materials, the SWNTs and fullerol particles passed through the porous medium more rapidly and to a greater extent than did the *n*-C_{60}. In aquatic systems, hydrophobic interactions may enhance the deposition of particles on surfaces. The surfaces of fullerenes are in principle quite hydrophobic and nonreactive in water. Indeed, fullerene hydrophobicity impedes the dispersal of materials such as buckyballs and carbon nanotubes in water. This barrier can be an important limitation in fullerene processing where dispersal or manipulation of fullerenes in aqueous solutions is required. The same hydrophobic forces

that prevent fullerene dispersal in water are also anticipated to lead to relatively limited mobilities in aquatic environments. However, fullerenes may become more hydrophilic through intentional or environmental modifications such as capping or wrapping of carbon nanotubes with surfactants (*21*) or the functionalization of C_{60} (*22*). Such modifications are anticipated to decrease attachment efficiency and thereby increase mobility. Consistent with these expectations, the solubilzed fullerene particles were relatively mobile. After approximately 2 pore volumes, the column effluent concentrations of SWNTs and fullerol particles were approximately 95% of those in the influent. By comparison, almost 50% of the 168 nm diameter *n*-C_{60} was removed from the flow thus, manifesting a much lower mobility.

Among the oxide nanomaterials, the smaller silica exhibited little affinity for the porous medium. With the exception of the metal oxanes, the passage of the other six nanomaterials tended to creep upward with time, suggesting a saturation or blocking of deposition sites within the porous medium. This observation suggests that mobility of these materials may increase over time as deposition sites become saturated over progressively larger distances within the porous medium. At the concentrations of the fullerol particles and SWNTs used in this work, porous medium surfaces were calculated to be covered as much as 6% by these materials after 1.5 pore volumes. Thus, plateau values of fullerene passage in these two cases may reflect some interactions between the nanomaterials and a modified silicate collector surface.

Estimates of particle attachment efficiency are obtained from the plateau values of C/C_0 using eq 2. The attachment efficiency provides one measure of nanomaterial mobility (Table 1). Although theoretical analyses assuming particle attachment in primary energy minima indicate that attachment efficiency should decrease with increasing particle size, experimental evidence, primarily using latex particles, typically indicates either little dependence on particle size or an increase in attachment efficiency with increasing particle size when conditions are unfavorable to attachment (*19*, *20*). The experimental attachment efficiency for the larger silica particles was over 1 order of magnitude larger than that of the smaller silica particles. In contrast with expectations based on electric double-layer interactions, this increase in attachment efficiency occurred despite an increase in surface potential as estimated from measurements of electrophoretic mobility.

Another means of expressing mobility can be obtained by re-arranging eq 2 to express particle mobility in terms of the distance L in a homogeneous porous medium that a suspension of nanoparticles would have to traverse to reduce their concentration to an arbitrary fraction of that initially present. This distance is calculated as a function of the experimentally determined values of the attachment efficiency and the value of C/C_0 selected. We have adopted a level of $C/C_0 = 0.001$ or a 3-log reduction in particle number concentration as a basis for calculating L as an index of nanoparticle mobility using values of flow, porosity, grain size, and temperature that might occur in an "ideal" groundwater aquifer(Table 1).

Consistent with the small values for attachment efficiency obtained for the polyhydroxylated C_{60} nanoparticles (fullerol) and surfactant-modified carbon nanotubes, comparatively high values for the mobility index are calculated for these materials. The calculated mobility indices for the initial transport of fullerol and surfactant-modified carbon nanotubes in a sandy aquifer are 10 m and 14 m for SWNTs and fullerol particles, respectively. The mobility index of the fullerol may be considerably greater than that suggested from a calculation of mean values of C/C_0 given that the estimate for the collision efficiency was not statistically different from zero (Table 1). For the conditions assumed in these calculations, groundwater would travel an approximate distance of 9 m in 1 day. Despite the very low initial solubility of untreated C_{60} particles in water, the stable suspension of *n*-C_{60} exhibited some mobility although its mobility index was nearly 140 times less than that of the fullerol. Similarly, the distance calculated for the SWNTs was appproximately 100 times greater than that calculated for the *n*-C_{60}. Thus, these aggregates of fullerenes exhibit relatively small mobilities in aqueous systems of homogeneous porous media.

Although the electrophoretic mobilities, sizes, and calculated mobilities of the *n*-C_{60} and the larger silica particles were similar, the evolution of their breakthrough curves differed. By comparison with the 135 nm silica particles, the *n*-C_{60} more rapidly approached the plateau value. Like the fullerol particles and SWNTs, the concentration of *n*-C_{60} reached a plateau value for removal within 2 bed volumes while the concentrations of oxide nanomaterials (with the exception of the ferroxane) continued to slowly increase after 3 bed volumes.

Currently, there are only a few known ongoing studies evaluating fullerene toxicity in aqueous systems. Due to the possibility of C_{60} solubilzation through colloid formation under environmental conditions, these studies have focused on the effects on *n*-C_{60}. The first known published work on *n*-C_{60} toxicity to organisms concluded that *n*-C_{60} produced oxidative damage in the brains of exposed largemouth bass (*23*). The results from the current study suggest that the potential for exposure to *n*-C_{60} through groundwater transport may be less than that of other fullerenes.

Numerous factors in natural systems may combine to increase nanoparticle mobility. For example, we speculate that naturally occurring polyelectrolytes such as fulvic and humic acids might create a similar enhancement in nanoparticle transport as that produced by the surfactant on the SWNTs by sorbing to the surfaces of particles and reducing attachment efficiencies through steric stabilization and increased hydrophilicity of the particle surface. Light- or bioactivated functionalization of C_{60} in nature may solubilize individual C_{60} molecules to yield molecules with very high mobilities similar to the fullerol examined in this work. Functionalization or clathrate formation may naturally induce *n*-C_{60} formation and confer moderate mobility in aqueous environments to these otherwise water-insoluble fullerenes. Moreover, while the porous medium used in these experiments was uniform and tightly packed, groundwater aquifers are likely to have fractures and other heterogeneities that may greatly enhance the mobility of particles beyond the values calculated in this work. Indeed, variability in the groundwater characteristics will introduce great variability in the mobility of particulate materials of all kinds.

Thus, the effects of naturally occurring organic matter associated with nanoparticles and collector surfaces, the evolution of collector surfaces with deposition as well as variations in solution chemistry, aquifer heterogeneity, and flow rate merit attention in future studies. The differences in the environmental transport properties observed for these nanomaterials underscores the need to address environmental impacts of nanomaterials on a case-by-case basis.

Acknowledgments

This research was supported in part by the Nanoscale Science and Engineering Initiative of the National Science Foundation under NSF Award EEC-0118007 and by the French Centre Nationale de la Recherche Scientifique (CNRS). We thank Dr. M. Wong for the use of ZetaPals Instrument and E. Corral and V. Murthy for conducting measurements.

Literature Cited

(1) Mize, S. *Nanotechnology Opportunity Report*; CMP Cientifica: March 2002.

(2) Zhang, W.; Wang, C. Nanoscale metal particles for dechlorination of PCE and PCBs. *Environ. Sci. Technol.* **1997**, *31* (7), 2154−2156.
(3) O'Melia, C. R. *Colloids Surf.* **1989**, *39*, 255.
(4) Happel, J. *AIChE J.* **1958**, *4*, 197.
(5) Derjaguin, B. V.; Landau, L. D. *USSR Acta Physicochim.* **1941**, *14*, 633.
(6) Verwey, E. J. W.; Overbeek, J. Th. G. *Theory of the Stability of Lyophobic Colloids*; Elsevier: Amsterdam, 1948.
(7) Rajagopalan, R.; Tien, C. *AIChE J.* **1976**, *22*, 523.
(8) Tufenkji, N.; Elimelech, M. Correlation equation for predicting single-collector efficiency in physicochemical filtration on saturated porous media. *Environ. Sci. Technol.* **2004**, *38*, 529−536.
(9) Yao, K. M.; Habibian, M. T.; O'Melia, C. R. *Environ. Sci. Technol.* **1971**, *5*, 1105.
(10) Adamczyk, Z. *J. Colloids Surf.* **1989**, *39*, 1.
(11) Veerapaneni, S.; Wiesner, M. R. *J. Environ. Eng.−ACSE* **1993**, *119*, 172.
(12) Tobiason, J. E.; O'Melia, C. R. *J. Am. Water Works Assoc.* **1988**, *80*, 54.
(13) Elimelech, M.; O'Melia, C. R. *Langmuir* **1990**, *6*, 1153.
(14) Elimelech, M. Effect of particle size on the kinetics of particle deposition under attractive double layer interactions. *J. Colloid Interface Sci.* **1994**, *164*, 190−199.
(15) Rose, J.; Cortalezzi-Fidalgo, M. M.; Moustier, S.; Magnetto, C.; Jones, C. D.; Barron, A. R.; Wiesner, M. R.; Bottero, J.-Y. *Chem. Mater.* **2002**, *14*, 621.
(16) Callender, R. L.; Harlan, C. J.; Shapiro, N. M.; Jones, C. D.; Callahan, D. L.; Wiesner, M. R.; MacQueen, D. B.; Cook, R.; Barron, A. R. *Chem. Mater.* **1997**, *9*, 2418.
(17) Scrivens, W. A.; Tour, J. M.; Creek, K. E.; Pirisi, L. *J. Am. Chem. Soc.* **1994**, *116*, 4517.
(18) Bronikowski, M. J.; Willis, P. A.; Colbert, D. T.; Smith, K. A.; Smalley, R. E. *J. Vacuum Sci. Technol. A* **2001**, *19*, 1800.
(19) O'Connell, M. J.; et al. *Science* **2002**, *297*, 593.
(20) Davis, S. N.; de Wiest, R. J. M. *Hydrogeology*; Wiley: New York, 1966.
(21) Smalley, R. E.; et al. *Abstr. Pap. Am. Chem. Soc.* **2001**, *221*, U555.
(22) Sawamura, M.; Nagahama, N.; Toganoh, M.; Hackler, U. E.; Isobe, H.; Nakamura, E.; Zhou, S.-Q.; Chu, B. *Chem. Lett.* **2000**, 1098.
(23) Oberdörster, E. *Environ. Health Perspect.* **2004**, *112*, 1058.

Received for review November 4, 2003. Revised manuscript received July 9, 2004. Accepted July 12, 2004.

ES0352303